

# TARGET DETECTION USING DYNAMICALLY RECONFIGURABLE SENSOR ARRAYS

Vijay Varadarajan and Jeffrey Krolik

Department of Electrical and Computer Engineering  
Duke University, Box 90291, Durham, NC-27708  
Email: {vv, jk}@ee.duke.edu

## ABSTRACT

This paper addresses the problem of target detection with multiple dynamically reconfigurable sensor arrays (DRSA's). The limited spatial coherence of the signal wavefront and dynamic nature of the interference seriously limit target detection performance. Traditional approaches to improve target detection include the use of large arrays with adaptive beamforming (ABF) or matched field processing (MFP) with static configurations. However, both these approaches suffer performance degradation in uncertain multipath environments when the training data is limited. Herein, we propose to improve the target detection performance by dynamically choosing the optimal orientation designed to maximize the array gain over a prescribed sector of bearing space for a DRSA based on the noise field directionality. Simulation results demonstrate the performance improvement obtained using the reconfiguring system as compared to a fixed uniform linear array (ULA) configuration with conventional or adaptive beamforming.

## 1. INTRODUCTION

The two major challenges faced by sensor arrays used for target detection are the suppression of highly dynamic interference and signal wavefront mismatch resulting from complex multipath propagation in uncertain channels which limits gain against diffuse noise. The use of conventional processing often proves to be inadequate due to the limited sidelobe rejection that is achievable [1]. ABF techniques [2] provide improved asymptotic performance but suffer degradation [3] due to the non-stationarity of the training data in dynamic interference environments. The conventional way to overcome the above difficulties has been to use larger array configurations which, in principle, can provide both greater gain against diffuse noise and more degrees of freedom for interference suppression. In practice, however, large static arrays often require even more accurate environmental information and greater noise field stationarity to minimize signal wavefront mismatch and facilitate the adaptation of more degrees of freedom. Moreover, in highly complex

multipath environments the spatial correlation length limits the array aperture that can be processed coherently. Another drawback using a fixed linear array with limited backlobe rejection is that interferers located close to the target backlobe can severely limit the array gain along the target direction due to the inherent left-right ambiguity associated with this configuration.

In this paper, DRSA's are proposed as a way of achieving the detection benefit of using more sensors without incurring the above difficulties. In this work, we propose a network of DRSA's which continually re-orient and translate themselves so as to collaboratively maintain maximum detection performance in an interference dominated uncertain multipath environment. Each DRSA is optimized for array gain for a hypothesized sector of bearing space as a function of the continually predicted noise directionality and detection performance. The target sectors to be optimized by the individual DRSA's depends upon the number of DRSA's deployed and modeled propagation conditions. Simulation results indicate that up to 30dB improvement in array gain is possible using a single DRSA for cases when the interferers are present close to the target back beam.

## 2. SIGNAL MODEL

In order to optimize reconfigurable arrays, consider a  $N$  element uniform linear array (ULA) with inter-sensor spacing  $d$  which samples the 2-D wavefield with components in  $k_x$  and  $k_y$ . In particular, the orientation of the ULA is defined by the angle  $\theta_{rot}$  in the horizontal plane with the  $x$  axis so that the coordinates of the  $n^{th}$  sensor are given by  $x_n(\theta_{rot}) = (n - 1)d \cos(\theta_{rot})$  and  $y_n(\theta_{rot}) = (n - 1)d \sin(\theta_{rot})$ . Denoting the column vector of sensor outputs at a given frequency corresponding to a wavelength  $\lambda$  by  $\mathbf{x} \in \mathbb{C}^{N \times 1}$ , we can write it's second order statistics as

$$\mathbf{R}_{xx} = \sigma_s^2 \mathbf{R}_s(\theta_s, \theta_{rot}) + \sigma_n^2 \mathbf{R}_n(\theta_{rot}) \quad (1)$$

where  $\mathbf{R}_{xx} = E \{ \mathbf{x} \mathbf{x}^H \}$ ,  $\mathbf{R}_s = \mathbf{d}(\theta_s, \theta_{rot}) \mathbf{d}^H(\theta_s, \theta_{rot})$ ,

$$[\mathbf{d}(\theta_s, \theta_{rot})]_n = e^{jd(k_x^s x_n(\theta_{rot}) + k_y^s y_n(\theta_{rot}))} \quad (2)$$

where  $[\cdot]_n$  denotes the  $n^{\text{th}}$  element of a vector, is the array response along the target direction,  $k_x^s = 2\pi \sin(\theta_s)/\lambda$  and  $k_y^s = 2\pi \cos(\theta_s)/\lambda$  are the 2 spatial frequency components and  $\mathbf{R}_n(\theta_{rot})$  is the noise covariance which is normalized such that  $\text{tr}(\mathbf{R}_n(\theta_{rot})) = N$ ,  $E\{\cdot\}$  refers to expectation and  $\text{tr}(\cdot)$  is the trace operator.

The noise covariance matrix  $\mathbf{R}_n(\theta_{rot})$ , which depends upon the array geometry, consists of 3 components which are uncorrelated with one another. The first component comprises of spatially uncorrelated receiver noise with covariance  $\mathbf{R}_e = \sigma_e^2 \mathbf{I}_N$  where  $\mathbf{I}_N$  is an  $N \times N$  identity matrix. The second component is due to far field interference sources whose directions are  $\boldsymbol{\theta}_{int} = \{\theta_1 \cdots \theta_p\}$ . The interference covariance matrix is given by

$$\mathbf{R}_{int}(\theta_{rot}) = \mathbf{D}(\boldsymbol{\theta}_{int}, \theta_{rot}) \mathbf{P} \mathbf{D}(\boldsymbol{\theta}_{int}, \theta_{rot})^H$$

where

$$\mathbf{D}(\boldsymbol{\theta}_{int}, \theta_{rot}) = [\mathbf{d}(\theta_1, \theta_{rot}) \cdots \mathbf{d}(\theta_p, \theta_{rot})]$$

and  $\mathbf{P} \in \mathbb{C}^{p \times p}$  contains the correlations between the different interferers and  $\mathbf{D}(\boldsymbol{\theta}_{int}, \theta_{rot}) \in \mathbb{C}^{N \times p}$  is the array response matrix to the interferers. We have dropped the dependence of  $\mathbf{R}_{int}$  on  $\boldsymbol{\theta}_{int}$  for notational expedience. Finally, platform noise which often occurs at end-fire and is independent of the array orientation has a covariance matrix given by

$$\mathbf{R}_e = \sigma_e^2 \mathbf{d}(\pi/2 - \theta_{rot}, \theta_{rot}) \mathbf{d}(\pi/2 - \theta_{rot}, \theta_{rot})^H$$

The noise covariance matrix can then be expressed as

$$\tilde{\mathbf{R}}_n(\theta_{rot}) = \mathbf{R}_e + \mathbf{R}_{int}(\theta_{rot}) + \mathbf{R}_e \quad (3)$$

from which we obtain  $\mathbf{R}_n = (N/\text{tr}(\tilde{\mathbf{R}}_n)) \tilde{\mathbf{R}}_n$  and  $\sigma_n^2 = \text{tr}(\tilde{\mathbf{R}}_n)/N$ .

The array gain which is defined as the ratio of the output signal-to-interference-plus-noise ratio (SINR) obtained using an array to that using a single sensor [3] is given by

$$g(\theta_s, \theta_{rot}) \triangleq \frac{\|\mathbf{w}^H \mathbf{d}(\theta_s, \theta_{rot})\|^2}{\mathbf{w}^H \mathbf{R}_n(\theta_s, \theta_{rot}) \mathbf{w}} \quad (4)$$

where  $\mathbf{w} \in \mathbb{C}^{N \times 1}$  is the array weight vector. The design of the DRSA in terms of  $\theta_{rot}$ , based on optimization of the array gain shall be discussed in the next section. Before describing the design of the DRSA, however, we shall point out some of the drawbacks associated with a static line array in terms of the measured field directionality. The field measured by a line array is a projection of the 2-D spatial spectrum with wavenumber components  $k_x$  and  $k_y$  related by  $k_x^2 + k_y^2 = (2\pi/\lambda)^2$  [4] (as shown in Fig. 1) onto the  $k_x$  line. The mainlobes for a set of contiguous beams measured by an array oriented along the  $x$  axis are illustrated by the

vertical stripe regions in Fig. 1. The limitations of a line array can be seen by noting that for this orientation, the target is completely masked by Interference 1 in the back-beam. Moreover, a further degradation of the field directionality estimate for this orientation occurs due to Interference 2 and 3 being spread in the projected sin-bearing space resulting in a loss of usable bearing space available for target detection.

### 3. DYNAMIC RECONFIGURABLE SENSOR ARRAY OPTIMIZATION

The key behind the DRSA concept stems from the fact that the orientations of multiple 1-D line arrays can be adaptively selected to optimally sample the 2-D wave field thereby taking different 1-D projections of 2-D (or 3-D) wavenumber space. The advantage of DRSA versus conventional moving or fixed arrays is thus that the observed projections of the 2-D wavenumber space can be dynamically optimized to maximize array gain for a hypothesized target direction, sector, or the entire isotropic field of view. This idea is illustrated by rotating the array by  $\pi/4$  in the scenario of Fig. 1. The resulting beams in the rotated projection in 2-D wavenumber space is shown in Fig. 2. Note that by changing the orientation of the array, Interference 1 been removed from the target back-beam and moreover Interferers 2 and 3 collapse into a single beam thereby substantially increasing the usable bearing space. This is somewhat analogous to finding the optimal scan orientation (projection) in tomographic imaging [5].

In this paper, the orientation of the DRSA is optimized as follows. Each DRSA is allocated a sector in bearing space over which surveillance must be performed to test for target presence. Let us denote this sector by  $\Theta_s$ . Using multiple DRSA's with different orientations, it is possible to reconstruct the 2-D wavenumber spectrum *approximately*, in that one can determine the sectors in bearing space from where the interferences arrive, as well as the approximate power levels of the interfering sources. Let us denote these quantities by  $\Theta_{int}$  and  $\hat{\sigma}_i^2(\theta)$  respectively. As shall be demonstrated in the simulation results, overestimation of the extent of interference sector  $\Theta_{int}$  or inaccurate estimation of the power level  $\hat{\sigma}_{int}^2(\theta)$  does not significantly impact the DRSA performance since these values are only used to choose an orientation and conventional processing is then performed on the data received by the optimally oriented array. An estimate of the background noise level  $\hat{\sigma}_e^2$  can be obtained from temporal frequencies or bearings wherein interfering sources are not present. An estimate of the noise level  $\hat{\sigma}_e^2$  due to the platform can be obtained during the design phase of the DRSA. Using the above estimates,

we form an estimated covariance matrix as

$$\hat{\mathbf{R}}_n(\theta_{rot}) = \int_{\theta_i \in \Theta_{int}} \hat{\sigma}_{int}^2(\theta_i) \mathbf{d}(\theta_{rot}, \theta_i) \mathbf{d}(\theta_{rot}, \theta_i)^H d\theta_i + \hat{\sigma}_e^2 \mathbf{I}_N + \hat{\sigma}_e^2 \mathbf{R}_e$$

From (5), we form an estimate of the array gain  $\hat{g}(\theta_s, \theta_{rot})$  for a conventional processor by substituting  $\hat{\mathbf{R}}_n = \tilde{\mathbf{R}}_n$  and  $\mathbf{w} = \mathbf{d}(\theta_s, \theta_{rot})$  in (4). Using  $\hat{g}(\theta_s, \theta_{rot})$ , we compute the optimal orientation for each DRSA as

$$\theta_{opt} = \arg \max_{\theta_{rot}} \int_{\theta_s \in \Theta_s} \hat{g}(\theta_s, \theta_{rot}) d\theta_s. \quad (5)$$

In other words, we pick the array orientation that maximizes the average array gain over the design sector  $\Theta_s$  under surveillance by the DRSA.

Since there is only one variable to optimize over, (5) can be carried out by a simple line search. In a general surveillance tasking, the orientation of different arrays within a group can be optimized for different sectors of bearing space. Although in this paper we focus on the optimization of each DRSA, collaboration among the arrays will serve to provide a unified dynamic model of the regional noise environment. The dynamic interference component of the noise can be fused with longer time-scale background noise model parameters and propagation loss assessments.

#### 4. SIMULATION RESULTS

To illustrate the array gain improvement that can be achieved with even a single DRSA array, consider the simulation scenario shown in Fig. 3 consisting of a weak target in the presence of 5 strong interferers. The input signal and noise variances were chosen such that  $\sigma_s^2/\sigma_n^2 = -24$  dB,  $\sigma_e^2/\sigma_n^2 = -30$  dB,  $\sigma_e^2/\sigma_e^2 = 20$  dB and  $tr(\mathbf{R}_{int}(\theta_{rot}))/(N\sigma_e^2) = 30$  dB. For comparison purposes, conventional beamforming with a fixed array oriented with broadside at  $0^\circ$  is compared with the array orientation which provides the maximum average array gain over all bearings, i.e.  $\Theta_s = [0, 2\pi)$ . The orientation of the DRSA array was optimized assuming the interference is in the shaded sector  $\Theta_{int} = [117^\circ, 243^\circ]$  which is a mismatched but reasonable model of the true interference locations, whose initial bearings which are given by  $\theta_{int} = \{112^\circ, 143^\circ, 162^\circ, 169^\circ, 189^\circ\}$  are shown in Fig. 3 indicating that there is one interferer that is outside the interference sector used in the optimization. The input SINR to compute the estimated array gain was set at 20 dB which is again mismatched with respect to the true value. The bearing versus time record (BTR) of a conventionally beamformed (CBF), fixed 20 element array at spacing  $2\lambda/5$  is shown in Fig. 4. Note that target at bearing  $\pi/4$  is completely masked by interferers in the back-beams. The BTR of the optimally oriented DRSA array is shown in Fig.

5. Note that the target at  $\pi/4$  is completely unmasked and the apparent interference bearings have been compressed into bearings beyond  $120^\circ$ . The unusable region near 0 degrees in Fig. 5 (as well as  $\pi/2$  in Fig. 4) represents the interference components that appear along the platform noise directions regardless of array orientation. A comparison of the array gain for CBF, clairvoyant ABF with the fixed array, and CBF for the DRSA array array is shown in Fig. 6. Note that the ideally-oriented DRSA offers about 30 dB improvement in array gain compared with the other approaches due to the latter's inability to mitigate interference that is in the ambiguous back-beam of the array.

#### 5. CONCLUSIONS

In this paper, we have presented an approach to use a dynamically reconfigurable sensor array to improve the detection performance compared to using conventional and adaptive beamforming with static configurations. The orientation of the DRSA is determined by optimizing the array gain over a desired target sector in bearing space. Simulation results suggest that significant improvement in terms of array gain as well as fraction of usable bearing space for target detection can be obtained using this approach.

#### 6. ACKNOWLEDGMENT

This work is supported by ONR. The authors would like to acknowledge the staff at Nekton Research LLC for useful discussions regarding the application of this concept.

#### 7. REFERENCES

- [1] H. Krim and M. Viberg, "Two decades of array signal processing research," *IEEE Signal Processing Magazine*, vol. 13, pp. 67–94, July 1996.
- [2] J. Capon, "High-resolution frequency-wavenumber spectrum analysis," *Proc. IEEE*, vol. 57, pp. 1408–1418, Aug 1969.
- [3] H. Cox, "An adaptive beamforming algorithm with simultaneous mainlobe response and tolerance sensitivity constraints," *Proc. 19th Asilomar conference on Sig. Sys. and Comp.*, pp. 565 – 569, Nov 1985.
- [4] D. H. Johnson and D. E. Dudgeon, *Array Signal Processing: Concepts and Techniques*. Prentice-Hall, 1993.
- [5] L. Shao, A. O. Hero, W. Rogers, and N. Clinthorne, "The mutual information criterion for the design and evaluation of spect apertures," *IEEE Trans. Medical Imaging*, vol. MI-8, pp. 322–336, Dec 1989.

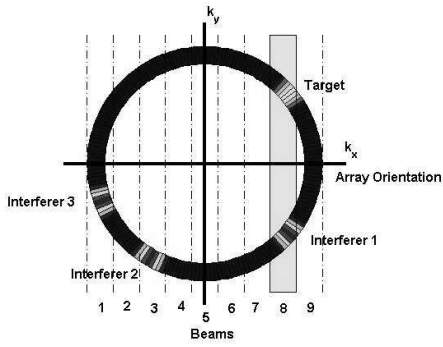


Fig. 1. 2-D frequency wavenumber spectrum for static ULA

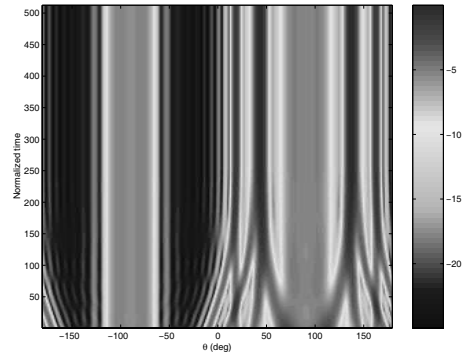


Fig. 4. Bearing time record using the static ULA

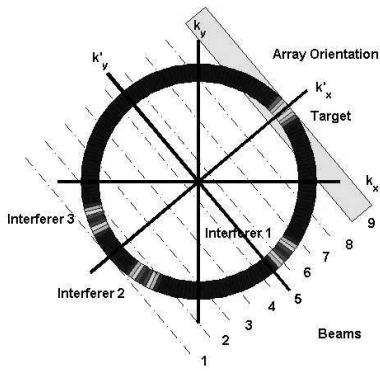


Fig. 2. 2-D frequency wavenumber spectrum for DRSA

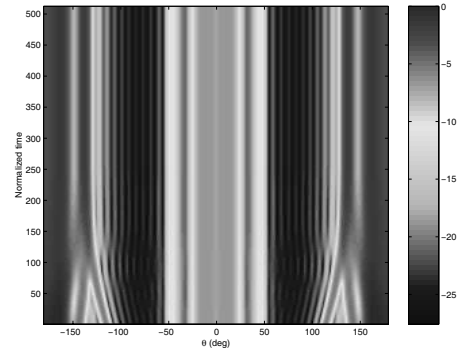


Fig. 5. Bearing time record using the DRSA

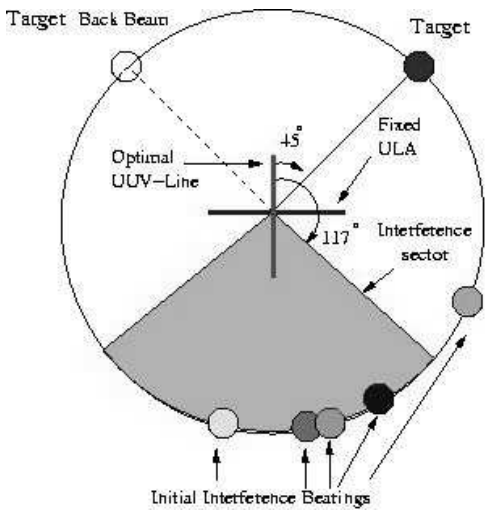


Fig. 3. Interference locations and the target sector

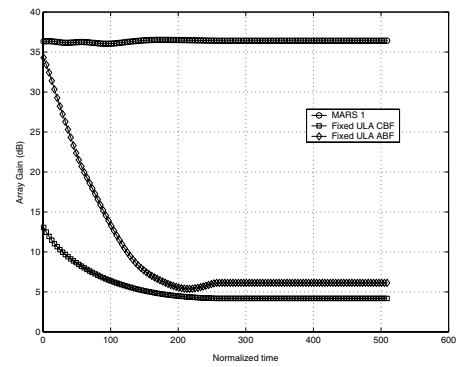


Fig. 6. Array gain (dB) for different configurations versus time